Initial stage of development of a high-pressure self-sustained microwave discharge in a plane-polarized field: elongation and stopping of the microwave streamer

P. V. Vedenin and N. E. Rozanov

Moscow Radio Engineering Institute of the Russian Academy of Sciences, 113519 Moscow, Russia
(Submitted 19 November 1993; resubmitted 17 January 1994)
Zh. Eksp. Teor. Fiz. **105**, 868–880 (April 1994)

The initial stage of a high-pressure self-sustaining microwave discharge is considered. The self-consistent two-dimensional dynamics of a microwave streamer in the field of a quasimonochromatic plane-polarized wave beam is investigated numerically, from an almost transparent symmetric plasma cloud to a plasmoid with length $l \approx 2\lambda/3$ elongated parallel to the external electric field (here λ is the wavelength). Analytical relations are obtained which exhibit possible reasons for the stopping of the microwave streamer.

1. INTRODUCTION

Aside from their possible applications, high-pressure microwave discharges are interesting and complicated objects of study in their own right. In the fully developed stage a microwave discharge (either triggered or self-sustaining) in a plane-polarized field is reminiscent of a formation moving in the opposite direction to the incident radiation and consisting of brightly emitting tangled elongated filaments primarily extended in the direction of the external magnetic field, separated by dark regions.[1,2]

A painstaking experimental study of a triggered microwave discharge reveals that a) the region where it exists can be broken up into structural zones within which the mechanism for the formation of the discharge structure and the nature of the propagation do not undergo any qualitative changes; b) in each structural zone we can distinguish a characteristic basis element of which the discharge as a whole is constructed.[3,4]

The general experimentally observed picture[2,5–7] of the development of a self-sustained microwave discharge from a discrete initiating ionization center is qualitatively the same in different gases and can be broken up into the following stages: 1) appearance of a quasispherical plasma cloud (plasmoid) about a discrete initial center of ionization; 2) elongation of the plasmoid (in this stage the plasma cloud assumes the form of an ellipsoid) parallel to the external electric field $\mathbf{E}_v$ until it reaches a size comparable with the wavelength λ of the infinite wave; 3) the development inside the plasmoid of one or several bright fine filaments extended in the direction parallel to $\mathbf{E}_v$; 4) growth of the filaments beyond the limits of the plasmoid and curvature of the filaments toward the source of the incident radiation, branching, and the development of the structure observed in the initial discharge (see above).

Stage 1, symmetric expansion of the quasispherical plasma cloud, continues until it becomes transparent to the incident electromagnetic radiation, i.e., as long as the condition $|\varepsilon-1| \ll 1$ holds, where ε is the dielectric constant of the plasma. In this stage the most important processes are impact ionization in the external electric field $\mathbf{E}_v$, attachment (in electronegative gases), and diffusion (initially free and then ambipolar). When the maximum plasma density in the center of the cloud reaches the value determined from the condition $|\varepsilon-1| \approx 1$, the role of the space-charge field becomes important. As a result the velocity with which the discharge propagates, which depends on the local values of the amplitude, turns out to be larger in the polar regions (the straight line connecting the poles of the quasispherical plasmoid, which is parallel to $\mathbf{E}_v$) than in the equatorial region. This is the reason for the elongation of the plasmoid in the direction parallel to the external electric field[6,8] (stage 2). In analogy with the similar phenomenon that occurs in a discharge in a static field (see, e.g., Ref. 9 and the works cited there) Gil'denburg *et al.*[10] referred to this elongating plasmoid as a high-frequency streamer. In Ref. 10 the evolution of a plasmoid in the electrostatic stage of elongation parallel to $\mathbf{E}_v$ was treated numerically in the two-dimensional approximation. In this model the effects associated with the finiteness of the wavelength λ of the incident electromagnetic radiation can be disregarded. Among other results Gil'denburg *et al.* noted the following: the magnitude of the field amplitude $|E_n|$ at the poles of the ellipsoid (and consequently the velocity of elongation) was considerably less than that which would have been expected based on the well-known formula (see, e.g., Ref. 11) $|E_n| = |\varepsilon|\,|E_i|$ for a uniform plasma ellipsoid. Here E_i is the field inside the ellipsoid, where $|E_i| \approx |E_v|$.

It is natural to associate the experimentally observed cessation of the plasmoid elongation parallel to the electric field with the substantial reduction in the field amplitude at the poles. The present work is devoted to finding the reasons for this effect. One such reason that we can immediately cite as a possibility is the finite radius of the wave beam. Specifically, in the elongation process the plasmoid inevitably enters the region where the external field becomes less than the breakdown field. If the space-charge field is strong, the microwave streamer ceases to grow. From this it follows that in studying the dynamics of the plasma formation we should not restrict ourselves to the electrostatic approximation. For our calculations and esti-

 1063-7761/94/040465-07$10.00

mates we have therefore chosen to use a two-dimensional electrodynamic model, to the description of which we now proceed.

2. EVOLUTION EQUATIONS FOR A MICROWAVE STREAMER

A plasmoid is located in the focal plane of a quasimonochromatic plane-polarized Gaussian wave beam, propagating in the x direction and having nonvanishing components B_z, E_y, E_x of the electromagnetic field (in the two-dimensional nonelectrostatic formulation we have $\partial(...)/\partial z\equiv 0$). The starting system of equations for complex amplitudes $\mathbf{A}(\mathbf{r},t)=1/2\,\mathbf{a}(\mathbf{r},t)e^{-i\omega t}+\text{c.c.}$ varying slowly in time $(\partial(...)/\partial t\ll\omega)$ takes the form

$$\left(\frac{\partial}{\partial x}\frac{1}{\varepsilon}\frac{\partial}{\partial x}+\frac{\partial}{\partial y}\frac{1}{\varepsilon}\frac{\partial}{\partial y}+1\right)B_z=0,$$

$$E_x=\frac{i}{\varepsilon}\frac{\partial B_z}{\partial y},\quad E_y=-\frac{i}{\varepsilon}\frac{\partial B_z}{\partial x},\tag{1}$$

where $kx,ky\rightarrow x,y$, $k=\omega/c$, $\varepsilon=1-n(1-i\nu)$, $\nu=\nu_e/\omega$, $n=n_e/n_c$, $n_c=m(\omega^2+\nu_e^2)/4\pi e^2$, $E_{x,y}/E_c\rightarrow E_{x,y}$, $B=B_z/E_c$, ν_e is the collisional momentum-transfer rate of the plasma electrons, m is the electron mass, n_e is the electron density, and E_c is the breakdown field. Here and in what follows we will always assume $\nu\gg 1$. In consequence of our stated goal, we have chosen for the description of the electron dynamics the simplest model equation that takes into account the following processes: impact ionization with frequency $\nu_i(|E|)$, attachment with frequency ν_a, ambipolar diffusion with coefficient D_a, and recombination with coefficient α_r. In addition we have assumed $\nu_i-\nu_a=\nu_a(|E|^\beta-1)$, and have taken ν_a, D_a, and α_r to be constants. In dimensionless variables this equation takes the form

$$\left[\frac{\partial}{\partial\tau}-|E|^\beta+1-D\left(\frac{\partial^2}{\partial x^2}+\frac{\partial^2}{\partial y^2}\right)+\alpha n\right]n=0,\tag{2}$$

where $\tau=\nu_a t$, $D=D_a k^2/\nu_a$, $\alpha=\alpha_r n_c/\nu_a$.

The solution of (1) in the symmetric expansion stage of an almost transparent ($|\varepsilon-1|\ll 1$) plasma cloud from a filamentary initial center with density $n(\tau=0,x,y)=n_\Sigma\delta(x)\delta(y)$, where $\delta(r)$ is a delta function, is given accurately by

$$n(\tau,r)=\frac{n_\Sigma}{4\pi D(\tau+T)}\exp\left(-\frac{r^2}{4D(\tau+T)}+\gamma(\tau+T)\right),\tag{3}$$

where we have written $r=\sqrt{x^2+y^2}$, $\gamma=|E|^\beta-1$, $|E|\approx|E_v|$, and $\mathbf{E}_v=\{E_{vx},E_{vy},0\}$ is the amplitude of the external field, which satisfies $|E_{vx}|\ll|E_{vy}|$. We have taken T to be the initial time. Expression (3) enables us to estimate the initial plasma parameters. Since the evolution of the plasmoid cannot depend sensitively on the choice of the initial density profile, we have assumed $\max\{n_0(\tau=0,r)\}=0.1/\nu$, $\gamma T=7$. Changing these initial parameters has practically no effect on the plasmoid dynamics for $\tau>1$.

Since the system is assumed to be symmetric about the x axis, we have

$$\frac{\partial B}{\partial y}(x,y=0)=0.\tag{4}$$

The boundary conditions imposed on surfaces $x=\pm x_m$, $y=y_m$ far from the plasmoid are a modified form of the Sommerfeld radiation condition appropriate to this problem:

$$\left[\frac{x}{R}\left(1+\frac{i}{2R}\right)+i\frac{\partial}{\partial x}\right](B-b^+e^{ix})\Big|_{x=\pm x_m}\approx 0,$$

$$\left(1+\frac{1}{2y}+i\frac{\partial}{\partial y}\right)(B-b^+e^{ix})\Big|_{y=y_m}\approx 0,\tag{5}$$

where $R=\sqrt{x_m^2+y^2}$, $b^+=B_v\Psi(x)\exp\{-(y\Psi(x)/a_f)^2\}$, $\Psi(x)=1/\sqrt{1+2ix/a_f^2}$, $B_v=E_v$, and a_f is the typical radius of the microwave beam in the focal plane. The expression for b^+ describes the wave amplitude profile in vacuum in the limit of a quasioptical beam $(\partial(...)/\partial x\ll 1)$.

To complete the formulation of the problem we note that Eqs. (1) and (2) remain valid under conditions such that T_v, $\nu_a|E|^\beta\ll\omega$, holds, where T_v is the time scale on which the amplitude B_v of the external field changes.

In order to solve Eqs. (1) and (2) with the initial and boundary conditions (4) and (5) we have written an implicit finite-difference scheme which is second-order accurate in x and y and first-order accurate in τ. To implement it we have developed the following algorithm: at each time step the equation for B is solved by coordinate timestep splitting, integrating until a steady value is reached; the evolution equation for $n(\tau,x,y)$ is integrated with a variable time step using an implicit scheme for the terms describing ionization, attachment, and recombination, and an explicit scheme for the terms describing diffusion. The accuracy of the calculations is ensured by checking energy conservation, which when we take into account the assumptions made above can be written in the form

$$G\equiv\nu\int_{D_*}d\xi d\eta n|E|^2$$

$$=\int_0^{y_m}d\eta[q_x(-x_m,\eta)-q_x(x_m,\eta)]-\int_{-x_m}^{x_m}d\xi q_y(\xi,y_m),\tag{6}$$

Here D_* is the region occupied by the plasma and we have written $\mathbf{q}=\mathrm{Re}[\mathbf{EB}^*]$. Equation (6) shows that the source of the plasma heating is the difference between the incident, transmitted, and reradiated energy.

3. RESULTS OF NUMERICAL SIMULATION

In this section we present the results of a numerical calculation with parameters $\beta=5.3$, $B_v=1.2$, $a_f=6$, $\nu=50$, $D=4\cdot 10^{-5}$, $\alpha=1.5$. This calculation is essentially of a methodological nature, although its motivation was to follow the initial stages of the evolution of a microwave streamer all the way to complete cessation of the elongation. We point out at the start that the energy conservation

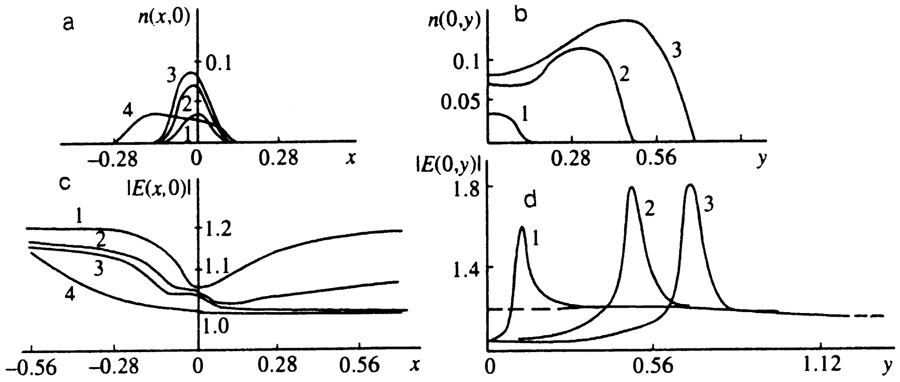

FIG. 1. Profile of the density n (a,b) and the field amplitude $|E|$ (c,d) in the x and y directions at times: *1)* $\tau=2.5$; *2)* 5.6; *3)* 7; *4)* 41. The vacuum field is shown by the broken trace.

(6) was maintained throughout the calculation to within at least 10%, and in the course of the streamer evolution the error decreased.

In Figs. 1–4 we have attempted to recreate the dynamics of a microwave streamer with as much clarity as possible, from a symmetric plasma cloud which is almost transparent to the incident radiation to a plasmoid elongated parallel to the external electric field to a length $l_y \approx \lambda/3$ and noticeably curved toward the radiation source. These figures show

1) the dynamics of the plasma density profile n and the magnitude $|E|$ of the electric field in the x and y directions (Fig. 1);

2) the shift in the boundaries [at the level $0.1n_m(\tau)$, where $n_m(\tau)$ is the maximum density at time τ) of the plasmoid toward the radiation source, denoted by l_x^- (trace *1*), and in the opposite direction, denoted by l_x^+ (trace *2*), and in the y direction, l_y (trace *3*), together with the time dependence of the power G absorbed by the plasma (trace *4*, Fig. 2);

3) how the field amplitude $|E(\tau,0,0)|$ decreases in time and the behavior of the maximum amplitude $|E(\tau)|_m$ at the head of the microwave streamer (Fig. 3);

4) contours of constant density in the xy plane at times $\tau=30$ and $\tau=40$ (Fig. 4).

The stage in which the plasmoid expands symmetrically ($\tau \leqslant 1$), during which $l_x^+(\tau) \approx -l_x^-(\tau) \approx l_y(\tau)$ holds and we have $|\varepsilon-1| \ll 1$, is replaced by preferential elongation in the y direction due to enhancement of the field at the poles (the plasma density profile is nonmonotonic in the y direction for the same reason). During times $1 \leqslant \tau \leqslant 7$ the density and the functions $V_y(\tau)=dl_y/d\tau$, $dG/d\tau$, $|E(\tau)|_m$ increase rapidly, and then for a short time $7 \leqslant \tau \leqslant 10$ they remain practically unchanged. This implies that the plasmoid lengthens at an almost constant rate while the $n(0,y)$ profile remains unchanged. Note that the results of our calculations and those given by Gil'denburg *et al.*[10] agree quite well (Ref. 10 was restricted to studying the evolution of the plasmoid in the stage corresponding to rapid increases in the discharge variables). A typical profile for the field amplitude $|E(x,0)|$ at time $\tau=5.6$ (trace 2 in Fig. 1c) shows that the asymmetry with respect to the Y axis is already quite pronounced, i.e., nonelectrostatic effects resulting from the treatment of the finite wavelengths have begun to show up.

At late times $\tau>10$: a) the rate at which the plasmoid lengthens slows down because the field amplitude $|E|_m$ at the poles decreases, and near the time $\tau \approx 42$ at which the calculation terminated the space-charge field is negligibly small in comparison with the vacuum field (the broken trace in Fig. 1d); b) the magnitude of the derivative $\partial n/\partial y$ which characterizes the curvature of the ionization wave front continually decreases; c) the loss power G increases only due to the increase in the size of the region D_* occupied by the plasma, but the growth rate $dG/d\tau$ drops off markedly and approaches zero for $\tau>40$; and d) the max-

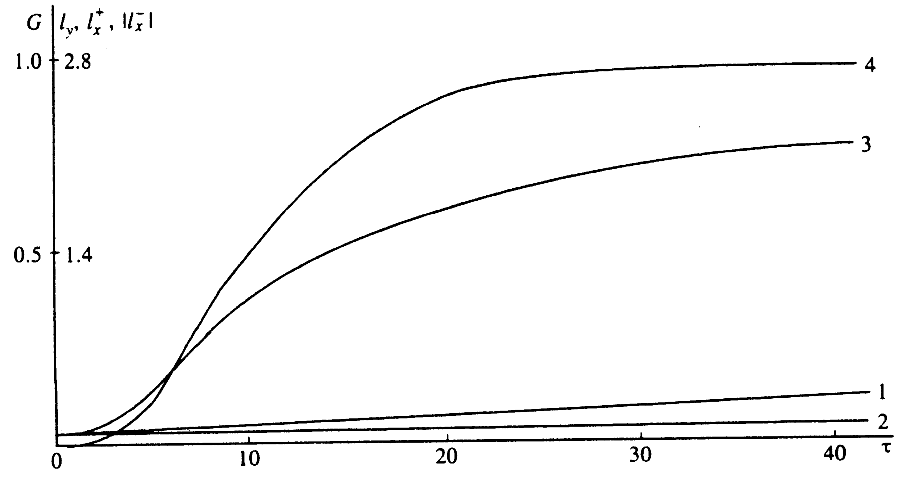

FIG. 2. Movement of the boundaries [at the level $0.1n(\tau)$] of the plasmoid opposite to and in the direction of the propagation of the incident wave (l_x^-, trace *1* and l_x^+, trace *2*, respectively), and in the direction of the electric field of the incident wave (l_y, trace *3*), along with the ohmic heating losses G in the plasma (trace *4*), as functions of time τ.

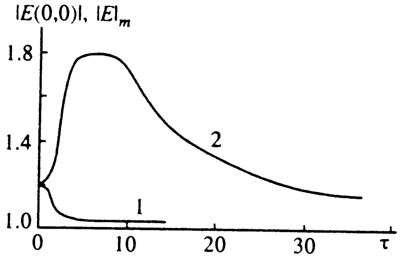

FIG. 3. Time dependence of the field amplitude $|E(0,0,\tau)|$ (trace *1*) and the maximum amplitude $|E|_m$ at the head of the streamer (trace *2*).

imum density $n_m(\tau)$ decreases. As can be seen from Fig. 2, when the plasma reaches length $l_y^{\max} \approx \lambda/3$ at times $\tau > 40$ it ceases to lengthen, but it continues to bend in the direction of the radiation source. We can estimate the extent of the deformation at late times from Figs. 1a and 1c (trace 4), and also from Fig. 4, where the $n(\tau,x,y)/n_m(\tau) = \text{const}$ contours are shown at times $\tau = 30$ and $\tau = 40$. Note that the quantity $l_y^{\max}$ and also the shape of the plasmoid agree reasonably well with the experimental data.[2,5,7]

And last but not least, as the quantity $L = l_y/l_x$ increases the effect of the concentrated space charge at the head of the streamer on the profile of the field amplitude in the x direction should weaken considerably, while the interaction of the electromagnetic wave with the plasmoid near this axis should increasingly resemble the interaction between a wave and a plane nonuniform plasma slab. In our opinion this is precisely what is proved by Fig. 1c, which shows the transformation of trace *1*, which is typical of the electrostatic limit (see the next section), into trace *4*.

To conclude this section we briefly summarize the main results and conclusions

1. Using our two-dimensional electrodynamic model we have performed a numerical simulation of the plasmoid dynamics, reproducing the experimentally observed stage in which the rate at which a microwave streamer lengthens in the direction parallel to the external fields decreases and finally stops entirely.

2. As shown by our analysis of the functions $l_y(\tau)$ and $|E(\tau)|_m$, in estimating the rate of elongation $V_y(\tau)$ of the microwave streamer we can use the asymptotic $(\tau \to \infty)$ solution V_{KPP} of the Kolmogorov–Petrovskii–Piskunov equation,[12] in which it is necessary to introduce a correction parameter q, i.e., to assume

$$V_y(\tau) \approx 2q\sqrt{D(|E(\tau)|_m^\beta - 1)}. \tag{7}$$

In the continuation of this calculation $(0 \leqslant \tau \leqslant 42)$ the quantity $q = V_y/V_{\text{KPP}}$ changed relatively slowly, $q = 1$–2. Expressions analogous to (7) can be written down also for $dl_x^\pm/d\tau$, but with $q \approx 1$.

3. The plasma density, the maximum field amplitude at the head of the beam, and the rate of elongation of the latter increased only during the electrostatic stage of the expansion, when finite-wavelength effects were negligibly small.

4. As in the calculations of Gil'denburg *et al.*,[10] the maximum amplitude at the head of the streamer was considerably less than might have been expected on the basis of the formula $|E|_m \approx |\varepsilon| E_v$, which is applicable to a uniform highly elongated $(L = l_y/l_x \gg 1)$ plasma ellipsoid.

4. INTERPRETATION OF THE RESULTS OF THE NUMERICAL SIMULATION

In this section we use a simple model of the plasma density profile inside the ellipsoid to propose answers to the following questions:

1. How does the typical curvature of the density profile affect the maximum field at the head of the microwave

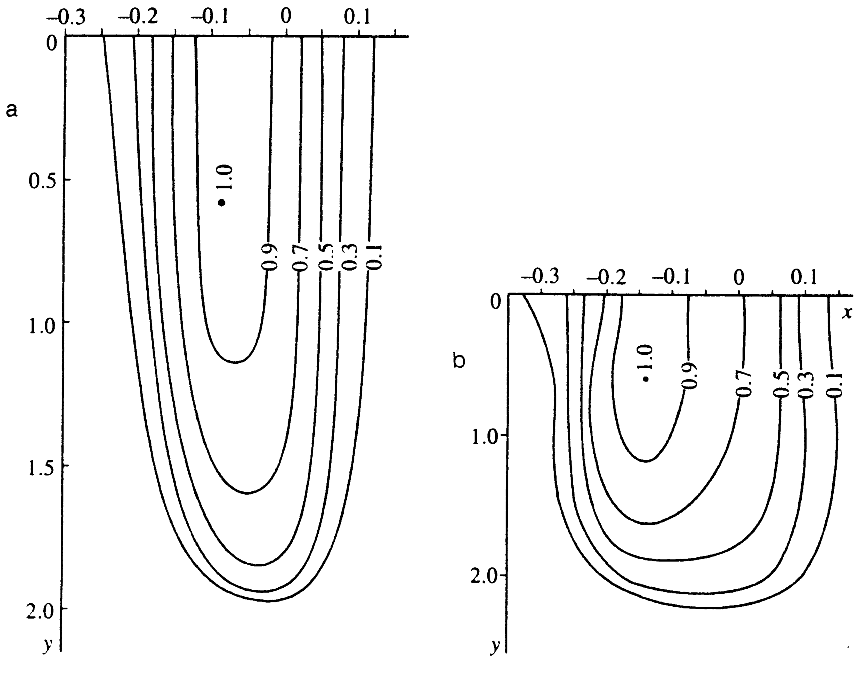

FIG. 4. Contours of constant plasma density $n/n_m(\tau) = \text{const}$ at times $\tau = 30$ (a) and $\tau = 40$ (b).

streamer and the profile of the electric field in the x direction in the electrostatic stage?

2. How is the originally symmetric plasma cloud deformed?

3. What are some possible reasons for the slowing down and stopping of the streamer?

The solution of the equation

$$\left(\frac{\partial^2}{\partial x^2}+\frac{\partial^2}{\partial y^2}+1\right)B^- = -\frac{4\pi}{\omega}\left(\frac{\partial j_y}{\partial x}+\frac{\partial j_x}{\partial y}\right) \tag{8}$$

for the amplitude B^- of the scattered field can be written down formally in integral form:

$$B^-(x,y,\tau)=\frac{i\pi}{\omega}\int_{D_*}\int d\xi d\eta\left[\frac{\partial j_y(\xi,\eta,\tau)}{\partial \xi} - \frac{\partial j_x(\xi,\eta,\tau)}{\partial \eta}\right]H_0^{(1)}(R), \tag{9}$$

where $H_0^{(1)}(R)$ is a Hankel function with argument $R = \sqrt{(x-\xi)^2+(y-\eta)^2}$, satisfying $H_0^{(1)}(R>1)\sim e^{iR}$, and $\mathbf{j}$ is the electron current density. Assuming that the scattered wave amplitude is small is comparison with the incident wave (recall that we are considering the case of a very dissipative plasma, $\nu\gg\omega$) and using perturbation theory, we can estimate the field amplitude in the regions of interest for a narrow ($l_x\ll 1$) plasmoid of arbitrary shape. The experimental data[2,5–7] and the results of numerical calculations[10] and the results given above imply that the shape of the microwave streamer is close to ellipsoidal, especially in the electrostatic stage of elongation. Based on this we have chosen the following model profile for the plasma density:

$$n=n_m\begin{cases}1, & S_0\leqslant S\leqslant 1,\\ S/S_0, & 0\leqslant S<S_0,\\ 0, & S<0,\end{cases} \tag{10}$$

where $S = 1 - x_*^2 - y_*^2$, $x_*=x/l_x$, $y_*=y/l_y$. The complicated expressions which give the distribution of the amplitude in the x and y direction in the electrostatic limit $l_y\ll 1$, $\sigma_* l_x\ll 1$, $\sigma_*=4\pi\sigma_m/\omega$, $\sigma_m=\omega_e^2(n_m)/4\pi\nu$, $\omega_e^2(n_m)=4\pi e^2 n_m/m$, in first order in perturbation theory are relegated to the Appendix. By analyzing these formulas in order to clarify the role of the curvature of the density profile, we reached the following conclusions.

1. The maximum amplitude is attained near the head of the streamer and can be estimated using the formula

$$|E|_m^2\approx|E(0,1)|^2 = |E_0|^2\left\{1+\frac{\sigma_*^2}{(L+1)^2}\left[1+\frac{\rho L^4}{(L+1)(L-1)^2}\times\left\{2[\sqrt{\rho^2(1-S_0)+1}-\rho]-\sqrt{S_0}\left(1-\frac{1}{L^2}\right)\right\}\right]^2\right\}, \tag{11}$$

where we have written $\rho = (L\sqrt{S_0})^{-1}$, so that in the limit $L\gg 1$ we have $\rho\approx\sqrt{r_0/2\Delta}$. Here $r_0=l_x^2/l_y$ is the radius of curvature of the head of the streamer, Δ is the typical thickness of the layer within which the density essentially goes to zero, and is related to the parameter S_0 by $S_0=(\Delta/l_y)(2-\Delta/l_y)$. In the limit $\rho\gg 1$ ($\Delta\ll r_0$) we arrive at the familiar formula for a uniform ellipsoid, $|E|_m\approx\sqrt{1+\sigma_*^2}|E_0|$ But if $\rho\ll 1$ and $\Delta\ll l_y$ hold, expression (11) simplifies and goes over to the following:

$$|E|_m^2\approx|E_0|^2(1+\Lambda^2), \tag{12}$$

where $\Lambda^2 = 2\sigma_*^2 r_0/\Delta$. Equation (12) shows that the maximum amplitude of the field in a highly elongated ($L\gg 1$) plasma ellipsoid with $r_0\ll\Delta$ is a function essentially only of a single parameter Λ.

2. The distribution of the field amplitude as a function of x, on the other hand, becomes gentler as the curvature of the density profile increases. This effect can easily be displayed at the points $(\pm 1,0)$. In fact,

$$|E(\pm 1,0,S_0=1)|=|E_0|\sqrt{1+\frac{\sigma_*^2}{(L+1)^4}} > |E(\pm 1,0,S_0=0)|=|E_0|.$$

This last relation implies that $|E(\pm 1,0,S_0)|$ decreases in the limit $S_0\to 0$. If $\sigma_*^2\ll(L+1)^4$ holds (and this condition is always satisfied), then we have $|E(\pm 1,0,S_0|\approx|E_0|$ for arbitrary S_0, i.e., the distribution of the field amplitude as a function of X is essentially independent of the curvature of the density profile.

3. As the distance from the plasmoid increases ($y_*\gg 1$, $x_*\gg L$, or y, $x\gg l_y$) the amplitudes

$$\begin{aligned}|E(0,y_*)|&\approx E_v\sqrt{1+\frac{\sigma_*^2(2-S_0)(L+1)}{4Ly_*^2[(L+1)^2+\sigma_*^2]}},\\ |E(x_*,0)|&\approx E_v\sqrt{1-\frac{\sigma_*^2(2-S_0)(L+1)L}{4x_*^2[(L+1)^2+\sigma_*^2]}},\end{aligned} \tag{13}$$

approach the value E_v from above and from below respectively and slightly affect the change in the parameter S_0.

Now, using the above relations, we proceed to a description of the electrostatic stage of elongation of a microwave streamer.

The stage in which the plasma cloud expands symmetrically from a filamentary initial point proceeds as long as $|\varepsilon-1|\ll 1$ holds and is determined [cf. Eq. (3)] by impact ionization in the field E_v and by attachment, along with diffusion (at first free and then ambipolar). As the density continues to grow the space-charge field becomes more and more important. The symmetric cloud begins to deform. This happens as follows. As the density increases the field near the plasmoid poles become stronger. This causes the $n(0,y)$ profile to become shallower at the center of the plasmoid and steeper at the poles. The increase in the typical density gradient in the y direction causes a further enhancement of the field near the poles, and so on. Thus, the process by which the symmetric plasma cloud is deformed in the direction of the external electric field resembles an instability related to the increase in the plasma density and its gradient. The curvature of the density profile $n(0,y)$ increases until diffusion begins to be important.

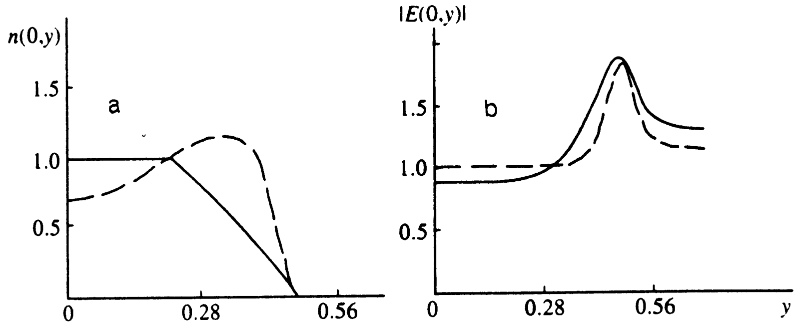

FIG. 5. Profiles of $n(0,y)$ (a) and $|E(0,y)|$ (b) calculated at time $\tau=5.6$ (broken trace) and obtained from the model (solid trace). The model field profile corresponds to the parameters $L=5$, $\sigma_*=5$, $S_0=0.8$.

There is practically no deformation in the x direction; this is because the profile of the field amplitude $|E(x,0)|$ becomes more gentle, while the profile of the density $n(x,0)$ becomes steeper in this direction. As a result of this process the density profile $n(x,0)$ even at the very beginning of elongation does not agree completely with the model profile (10). However, as was already pointed out, if the ratio $\sigma_*^2/(L+1)^4$ is small (and this condition is easy to satisfy), then the distribution of the field amplitude as a function of x is essentially independent of S_0. This implies that in approximating the calculated curves $|E(x_*,0)|$ we can use relation (A.2) (see Appendix) with $S_0=1$.

As the plasmoid evolves the quantity σ_* reaches a maximum value at $\tau=7$ (the rise in the density is limited by the decrease in $|E_0|$, recombination, and diffusion in the x direction), the curvature in the density profile $n(0,y)$ changes little, and the ratio L of the lengths of the axes of the ellipsoid increases. Consequently Λ and along with it V_y decreases for $\tau>7$. Based on this we can deduce that similar variations in both the plasmoid density and its shape are a second possible reason for the slowing down of the microwave streamer (the first one was mentioned in the Introduction).

Figure 5 presents the analytical treatment of the electrostatic stage, showing how well our formulas work. It displays the calculated (broken trace) and model profiles of the density $n(0,y)$ (Fig. 5a), and also the corresponding amplitude profiles $|E(0,y)|$ (Fig. 5b) at time $\tau=5.6$. As can be seen, despite the considerable discrepancy in the density profiles the amplitude profiles show good agreement. It should not be forgotten that this result was obtained using only first-order perturbation theory.

As it lengthens the plasma goes over to the nonelectrostatic stage in which $l_y>1$ holds; in estimating the magnitude of $|E|_m$ in this case we must not only take into account the space-charge field from the immediate vicinity of the head of the streamer in Eq. (9), but also the interference of waves emitted by more distant oscillators. The boundary between the electrostatic and wave regions of the plasmoid is very provisional and is related in a purely mathematical fashion to the various asymptotic forms of the Hankel function:

$$H_0^{(1)}(z)\approx\begin{cases}\dfrac{2i}{z}\ln\dfrac{z}{2}, & |z|\ll 1,\\[2mm] \sqrt{\dfrac{2}{\pi z}}\exp\left[i\left(z-\dfrac{\pi}{4}\right)\right], & |z|\gg 1.\end{cases}$$

In our calculations the nonelectrostatic phase of elongation begins at $\tau\approx 10$.

The results of the numerical simulation show how strongly the plasmoid is deformed for $\tau>10$ (see, e.g., Fig. 4). However, using the model density profile (10) with $S_0=1$ we have tried to estimate the maximum field amplitude at the head of the beam anyway, assuming that such an estimate can give a qualitative picture of the evolution of $|E|_m$ in the electrodynamic stage when $l_y>1$ holds. The expression for $|E|_m$ takes the form

$$|E|_m\approx B_0\exp\left[-\left(\frac{l_y}{a_f}\right)^2\right]\sqrt{\left(1-\frac{\Delta F}{2}\right)^2+\frac{\Delta^2\Phi^2}{4}},\qquad(14)$$

where

$$F(l_y)=\frac{1}{3}\sqrt{\frac{2}{\pi l_y}}\int_1^{2l_y}dz\left(2-\frac{z}{l_y}\right)^{3/2}\sin\left(z-\frac{\pi}{4}\right)$$

and

$$\Phi(l_y)=\frac{5\sqrt{2l_y-1}}{3\pi l_y}$$

are the contributions of the wave and electrostatic regions of the plasmoid respectively to $|E|_m$. The function $F(l_y>1)$ rises to a maximum value $F_m(l_y\approx 3)\approx 0.4$, and then drops off, oscillating weakly. But the function $\Phi(l_y)$ falls off monotonically, and $\Phi(l_y\geqslant 3)\approx F(l_y\geqslant 3)$. Analysis of Eq. (14) allows us to infer that the rate at which the plasmoid lengthens subsequently decreases as it moves to the nonelectrostatic stage. Furthermore, wave effects (the term $-\Delta F/2<0$) can probably reduce $|E|_m$ to a value below the vacuum field amplitude and shut off the elongation of the plasmoid even where the vacuum field is above breakdown.

Thus, the high-frequency streamer elongation can slow down and stop due to 1) the drop in the field at the head of the plasmoid due to the finite size of the focal spot of the incident radiation; 2) the change in the shape of the streamer when the plasma density is approximately constant in time [cf. Eq. (12)]; or 3) wave effects which lead to a decrease in the field at the head of the streamer to values below the vacuum level during the nonelectrostatic stage.

5. PRINCIPLE RESULTS AND CONCLUSIONS

We have developed a numerical algorithm which enables us to treat the two-dimensional evolution of a microwave streamer in the linearly polarized field of a wave beam of finite radius as it goes from a symmetric, almost transparent plasma cloud to a plasmoid elongated parallel to the electric field with length $l_y \approx 2\lambda/3$. These results reproduce experimental data in a qualitative fashion. We have found a connection between the rate at which the streamer lengthens and the maximum field amplitude at the head. We have shown that the plasma density, the maximum amplitude of the field, and the rate of elongation grow only in the electrostatic stage of the process.

Using the model of a nonuniform plasma ellipsoid we have obtained simple analytical expressions which yield the profile of the field amplitude in the x and y directions, and also show that (and actually show how) the field amplitude at the poles depends on the maximum density, the characteristic curvature of the density profile, and the aspect ratio of the ellipsoid. We have used these relations to exhibit possible reasons for the decrease in the rate of elongation of the streamer in the direction of the electric field and why it stops. These are related to a) the finite radius of the wave beam; b) the change in the shape of the plasmoid (elongation when the maximum density is approximately constant and the characteristic profile parallel to the field does not change); and c) nonelectrostatic effects.

In this work we have omitted from consideration processes associated with the heating of the gas, which can give rise to experimentally observable brightly emitting filaments within the plasmoid, through the mechanism of the thermal instability (see Introduction). Hence in the next stage of these investigations it is proposed to consider the evolution of a plasmoid, taking into account gas heating and a number of plasma-chemical reactions.

We thank G. M. Batanov, L. P. Grachev, Yu. F. Kolesnichenko, I. A. Kossoi, and K. V. Khodataev for their interest in this work and for fruitful discussions.

APPENDIX

The expressions for the distribution of the field amplitudes in the x and y directions derived for the model plasma density profile (10) take the form

$$\frac{|E(0,y_*)|^2}{|E_0|^2}=\begin{cases}1, & y_*\leqslant\sqrt{1-S_0},\\ \dfrac{1}{|\varepsilon(0,y_*)|^2}\left\{1+\dfrac{\sigma_*^2}{(L+1)^2}\left\{1+\dfrac{L}{(L+1)S_0}\left[1+(1-y_*^2)L-\dfrac{L^2}{(L-1)^2}(y_*-Q(S_0))^2\right]\right\}^2\right\}, & \sqrt{1-S_0}\leqslant y_*\leqslant 1,\\ 1+\dfrac{\sigma_*^2}{(L+1)^2}\left\{1+\dfrac{L^3}{(L^2-1)(L-1)S_0}\left[2y_*(Q(S_0)-Q(S_0=0))-\left(1-\dfrac{1}{L^2}\right)S_0\right]\right\}^2, & y_*\geqslant 1,\end{cases} \tag{A1}$$

$$\frac{|E(x_*,0)|^2}{|E_0|^2}=\begin{cases}1, & x_*\leqslant\sqrt{1-S_0},\\ \dfrac{1}{|\varepsilon(x_*,0)|^2}\left\{1+\dfrac{\sigma_*^2}{(L+1)^2}\left\{1+\dfrac{L}{S_0}\left[1-\dfrac{L+2}{L+1}x_*^2+\dfrac{1}{(L^2-1)(L-1)}(x_*-R(S_0))^2\right]\right\}^2\right\}, & \sqrt{1-S_0}\leqslant x_*\leqslant 1,\\ 1+\dfrac{\sigma_*^2}{(L+1)^2}\left\{1+\dfrac{L}{(L^2-1)(L+1)S_0}[-(L^2-1)S_0+2x_*(R(S_0=0)-R(S_0))]\right\}^2, & x_*\geqslant 1,\end{cases} \tag{A2}$$

where

$$Q(S_0)=\sqrt{y_*^2-(1-S_0)\left(1-\frac{1}{L^2}\right)},$$

$$R(S_0)=\sqrt{(L^2-1)(1-S_0)+x_*^2},$$

and

$$E_0=E_y/[1+i\sigma_*/(L+1)].$$

We emphasize that the quantity $1/(1+L)$ in the expression for E_0 agrees closely with the corresponding depolarization coefficient of a uniform ellipsoid. This is the reason for assuming that in the plateau region of the density, i.e., for $S_0\leqslant S\leqslant 1$ (in the central part of the plasmoid) this formula for the amplitude is exact.

[1] G. M. Batanov, S. I. Gritsinin, I. A. Kossyi *et al.*, Trans. FIAN **160**, 174 (1985).
[2] L. P. Grachev, I. I. Esakov, F. I. Mishin *et al.*, Zh. Tekh. Fiz. **50**, 149 (1989) [Sov. Phys. Tech. Phys. **34**, 1181 (1989)].
[3] V. G. Brovkin and Yu. F. Kolesnichenko, Pis'ma Zh. Tekh. Fiz. **16** (2) 55 (1990) [Sov. Tech. Phys. Lett. **16** 107, (1990)].
[4] V. G. Brovkin and Yu. F. Kolesnichenko, Pis'ma Zh. Tekh. Fiz. **17** (1), 58 (1991) [Sov. Tech. Phys. Lett. **17**, 22 (1991)].
[5] L. P. Grachev, I. I. Esakov, G. I. Mishin, and K. V. Khodataev, Preprint No. 1577, Ioffe Physicotechnical Institute, St. Petersburg (1992).
[6] A. L. Vikharev, V. B. Gil'denburg, O. A. Ivanov *et al.*, Fiz. Plazmy **12**, 1503 (1986) [Sov. J. Plasma Phys. **12**, 870 (1980)].
[7] A. L. Vikharev, A. M. Gorbachev, A. V. Kim *et al.*, Fiz. Plazmy **18**, 1064 (1992) [Sov. J. Plasma Phys. **18**, 554 (1992)].
[8] S. A. Dvinin, Vestn. MGU, Ser. 3, Fiz., Astron. **26**, 30 (1985).
[9] É. D. Lozanskii and O. B. Firsov, *Theory of the Spark* [in Russian], Atomizdat, Moscow (1975).
[10] V. B. Gil'denburg, I. S. Gushchin, S. A. Dvinin *et al.*, Zh. Eksp. Teor. Fiz. **97**, 1151 (1990) [Sov. Phys. JETP **70**, 645 (1990)].
[11] L. D. Landau and E. M. Lifshits, *Electrodynamics of Continuous Media*, Pergamon Press, Oxford (1982).
[12] A. N. Kolmogorov, I. G. Petrovskii, and N. S. Piskunov, in *Topics in Cybernetics, Vol. 12* [in Russian], Izd. AN SSSR, Moscow (1975).

Translated by David L. Book